# Feedback Stabilization of Multiple Resistive Wall Modes

P. R. Brunsell,[1] D. Yadikin,[1] D. Gregoratto,[2] R. Paccagnella,[2] T. Bolzonella,[2] M. Cavinato,[2] M. Cecconello,[1] J. R. Drake,[1] A. Luchetta,[2] G. Manduchi,[2] G. Marchiori,[2] L. Marrelli,[2] P. Martin,[2] A. Masiello,[2] F. Milani,[2] S. Ortolani,[2] G. Spizzo,[2] and P. Zanca[2]

[1]*Division of Fusion Plasma Physics (Association EURATOM/VR), Alfvén Laboratory, Royal Institute of Technology, 10044 Stockholm, Sweden*

[2]*Consorzio RFX, Associazione EURATOM-ENEA sulla Fusione, 35127 Padova, Italy*

(Received 22 June 2004; published 22 November 2004)

Active feedback stabilization of multiple independent resistive wall modes is experimentally demonstrated in a reversed-field pinch plasma. A reproducible simultaneous suppression of several nonresonant resistive wall modes is achieved. Coupling of different modes due to the limited number of the feedback coils is observed in agreement with theory. The feedback stabilization of nonresonant RWMs also has an effect on tearing modes that are resonant in the central plasma, leading to a significant prolongation of the discharge pulse.

DOI: 10.1103/PhysRevLett.93.225001 PACS numbers: 52.55.Tn, 52.30.Cv, 52.35.Py, 52.55.Hc

Stabilization of ideal magnetohydrodynamic kink modes with a close conducting wall is currently pursued in advanced tokamaks operating at high beta [1]. Absent plasma rotation, the kink mode is not completely stabilized, but rather converted into an unstable resistive wall mode (RWM) with a growth time comparable to the wall magnetic flux penetration time. In the tokamak, the RWM can be either passively stabilized by fast plasma rotation or actively suppressed by magnetic feedback control [2,3]. The reversed-field pinch (RFP) is a toroidal axisymmetric configuration, similar to the advanced tokamak, in the sense that it uses a conducting wall for kink mode stabilization. The physical model, incorporating a thin wall, used for determining RWM stability and growth, is the same for the tokamak and the RFP [4–6]. However, since the RFP differs from the tokamak in that the poloidal and toroidal magnetic fields are of the same order of magnitude, the RFP has a different RWM spectrum and, in general, a range of modes are unstable. Therefore, the requirement of simultaneous feedback stabilization of multiple independent RWMs arises for the RFP configuration.

Simultaneous feedback stabilization of multiple modes has been studied theoretically [7–11]. The additional complication that arises with multiple modes is primarily the possible coupling of unstable modes through the feedback coils. The origin of the coupling is the generation of ''sideband'' harmonics by the feedback coils. This is a general characteristic of any feedback coil system and, therefore, the issue is also important for other configurations than the RFP. In practical terms, the need to avoid coupling of modes puts a constraint on the minimum number of active coils in the arrays.

The main RWMs in the RFP are intrinsic, nonresonant, current-driven kink modes that are largely unaffected by sub-Alfvénic plasma rotation [4–6]. A range of RWMs with poloidal mode number $m = 1$ having different toroidal mode number $n$ is unstable at a given time. In the RFP, it is possible to measure and selectively feedback control individual RWMs by using arrays with many active coils distributed along the toroidal direction. RWMs have been observed earlier in thin shell RFP experiments as nonrotating, growing magnetic perturbations [12,13]. Active feedback suppression of a single RWM using helical windings has been demonstrated in the HBTX-1C device [14].

The present results, obtained in a reversed-field pinch configuration, are the first experimental demonstration of simultaneous feedback stabilization of multiple independent RWMs. A reproducible suppression of several nonresonant RWMs is achieved through direct feedback action. According to theory, the number of feedback coils in the toroidal direction limits the range of modes that can be simultaneously stabilized [8]. In the present experiment, coupling due to the limited number of coils is observed, in agreement with the theory prediction. The feedback stabilization of nonresonant RWMs also has an effect on tearing modes that are resonant in the central plasma. The reduction of RWM amplitudes leads to a delay in the braking of the plasma rotation, as measured by the tearing mode rotation, resulting in a significant prolongation of the discharge pulse.

The experimental device used is the EXTRAP T2R RFP (major radius $R = 1.24$ m, plasma limiter minor radius $a = 0.183$ m) [15]. The plasma is surrounded by a close-fitting conducting wall, or thin shell, at a normalized radius $r/a = 1.08$, with a vertical magnetic field penetration time of $\tau_w = 6.3$ ms. The shell is modeled using the ''thin shell approximation'' since the skin depth in the wall material for the RWMs is much larger than the wall thickness. The plasma current in the present experiments is around $I_p = 80$ kA and the discharge length is

 © 2004 The American Physical Society

15–23 ms, equivalent to 3–4 wall times. The magnetic equilibrium is to a first order characterized by the parameter $\Theta = B_\theta(a)/ < B_\phi > = 1.65$, where $B_\theta(a)$ is the poloidal field at the wall and $< B_\phi >$ is the cross-section average of the toroidal field. A range of nonlinearly saturated $m = 1$ tearing modes, resonant in the central plasma, are intrinsic to the RFP configuration. For the present equilibrium, these modes have toroidal mode numbers $n \leq -12$. ($n < 0$ is used for modes with the same helical handedness as the equilibrium field in the central plasma.) The plasma has a fast spontaneous toroidal rotation, and typically, the saturated tearing modes are co-rotating with the plasma at high angular frequencies that significantly exceed the inverse wall time [16,17]. As a consequence, the main tearing modes largely behave as if the wall were ideally conducting. The two main groups of unstable $m = 1$ RWMs are internally nonresonant modes $-11 \leq n \leq -3$ and externally nonresonant modes $+1 \leq n \leq +7$. The experimental growth rates of the main RWMs, measured with an array of flux loops (described below), are in quantitative agreement with circular, straight-cylinder linear MHD model calculations (Fig. 1) [18]. The internally nonresonant modes $n = -10, -11$ have the highest growth rates, in agreement with theory. The $-2 \leq n \leq +2$ modes have experimentally higher growth rates than predicted. The fast growth of these low-$|n|$ modes is believed to be related to magnetic field errors due to machine asymmetries.

The actuator part of the RWM feedback stabilization system is an array of saddle coils placed at a radius $r/a = 1.28$ outside the shell, shown schematically in Fig. 2. Each coil, with 40 turns, extends 90° poloidally and $360/32 = 11.25°$ toroidally. The coverage in the poloidal direction is complete with $M_c = 4$ coils, while partial in the toroidal direction, with $N_c = 16$ equally spaced poloidal arrays that cover 50% of the toroidal circumference. The four coils at a toroidal position are hard-wired into two pairs forming one $m = 1$ "cosine coil" (outboard to inboard) and one $m = 1$ "sine coil" (top to bottom). The $m = 1$ connected coil has an $L/R$ time of $\tau_c = 1$ ms. It is driven with a high-bandwidth audio amplifier ($f_c = 25$ kHz, satisfying $f_c \gg \tau_c^{-1}, \tau_w^{-1}$), producing a maximum current of 20 A corresponding to a magnetic field at the wall of the order of $B_c = 1$ mT, about 1% of the equilibrium poloidal field. The sensors are single turn flux loops placed inside the shell with 90° poloidal angular widths (same as active coils) and $360/64 = 5.625°$ toroidal angular width (half the active coil width), measuring the local radial magnetic flux through the shell. There are $M_s = 4$ coils in the poloidal direction and $N_s = 32$ equally spaced poloidal arrays of sensor coils in the toroidal direction. The sensor coils are pair connected into $m = 1$ cosine and sine coils, similar to the active coils. A digital controller that has been developed for the reversed field experiment (RFX) is used [19,20]. It receives inputs from $2 \times 32 = 64$ sensor signals and computes in real time the toroidal Fourier mode decomposition of the radial field. The $m = 1$ modes resolved are $-15 \leq n \leq +16$ that includes all RWMs as well as the main resonant tearing modes. Each mode, characterized by the toroidal mode number $n$, is then separately feedback controlled using a specific proportional feedback gain set for the mode. The inverse Fourier transform is computed and $2 \times 16 = 32$ output voltages to the active coil amplifiers are produced. The cycle time for the digital controller is 100 $\mu$s. Setting the feedback gains for all modes equal results in feedback action that attempts to maintain zero flux through all the sensor coils, the so called intelligent shell scheme [7]. The open loop proportional gain, defined as the ratio of the sensor flux produced by the coil current to the sensor flux measured, is $G_0 = 2.5$, (at low frequency, $f \ll \tau_c^{-1}, \tau_w^{-1}$, without plasma), which is sufficient for achieving cancellation of about 90% of the sensor flux in the present experiment.

The discrete array of active coils gives rise to a coupling of modes through the feedback action. Coil currents corresponding to a toroidal harmonic $n_c$ produce a radial field composed of several Fourier harmonics $n_f = n_c + iN_c$, where $i = \ldots -2, -1, 0, +1, +2, \ldots$ (Fig. 3). The sensor array resolves two modes in each set. As an ex-

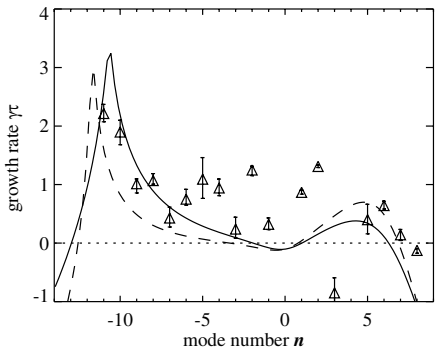


FIG. 1. Experimental $m = 1$ RWM growth rates vs toroidal mode number $n$ for $\Theta = 1.65$. Linear MHD calculation are shown for $\Theta = 1.55$ (solid line) and $\Theta = 1.78$ (dashed line). Growth rates normalized to the long wall time ($\tau = \mu_0 \sigma b d = 13.8$ ms, $\tau \approx 2\tau_w$).

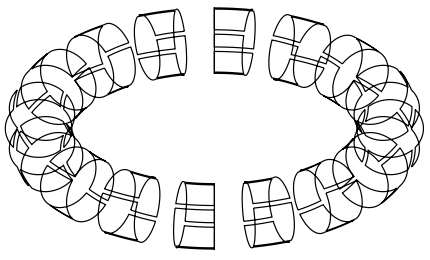

FIG. 2. Schematic drawing of the active coil layout on the torus showing the 16 toroidal positions with four saddle coils, each coil spanning $\theta = 90°$ poloidally and $\phi = 11.25°$ toroidally.

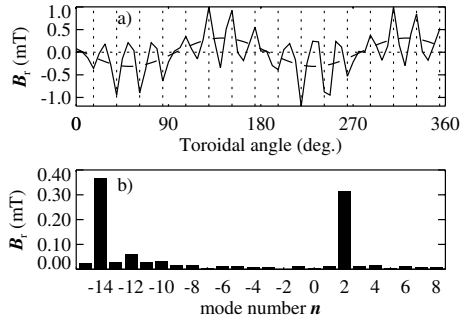


FIG. 3. Preprogrammed $n_c = +2$ coil current (without plasma). Field harmonics $n = (-14, +2)$ are produced by the active coil array. (a) Toroidal distribution of $m = 1$ field (solid line), $n = +2$ harmonic (dashed line); vertical lines indicate toroidal positions of active coils. (b) Toroidal $m = 1$ mode spectrum corresponding to field in (a).

ample, consider feedback suppression of a plasma mode $n = -10$. The control system responds with a $n_c = -10$ coil current harmonic that produces control field harmonics $n_f = (-10, +6)$, thereby coupling the plasma modes $n = (-10, +6)$. There is also a coupling of low-$|n|$ modes and modes that are resonant in the central plasma. Feedback acting on the $n = +2$ mode produces a $n = -14$ harmonic that interacts with the corresponding resonant tearing mode. In these experiments, feedback suppression of the modes $-2 \le n \le +2$ is removed in order to avoid negative effects on rotating tearing modes as well as on the equilibrium vertical field.

The time evolution of the radial field amplitudes for the main RWMs are shown in Fig. 4. Three cases are shown, one case without feedback, and two cases with feedback. The cases with feedback differ in the selection of modes targeted for feedback. The magnitude of the coil currents in the present experiments is well below the maximum current limit. In the first feedback case (dashed line), the same proportional gain is set for modes $-15 \le n \le +16$ (except for modes $-2 \le n \le +2$). With feedback, the growth of the dominant internally nonresonant unstable RWMs $-11 \le n \le -8$ is reduced. The main internal nonresonant RWMs ($n = -11, -10$) are both partially suppressed. The phases of the modes are shot-to-shot reproducible and depend on initial conditions determined by field errors during discharge start-up. As a result of the feedback, a reproducible extension of the pulse is observed. If the low-$n$ modes are also included, the suppression of the main RWMs is similar but the discharge prolongation is less.

Feedback action with the present coil array couple several pairs of unstable RWMs, $n = (-11, +5)$, $n = (-10, +6)$ and $n = (-9, +7)$. The internal nonresonant modes have the highest growth rates in each set for the present equilibrium, and will be the primary modes mainly determining the amplitude and phase of the control field. The initial suppression of the secondary externally nonresonant coupled modes is different for the two

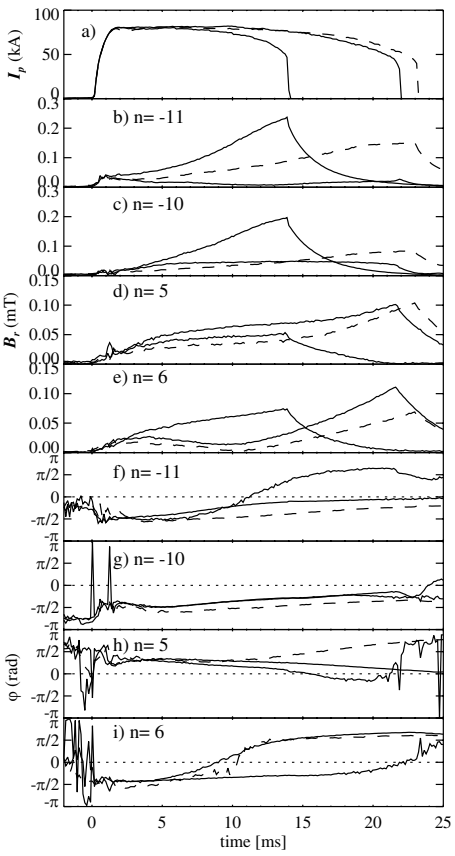


FIG. 4. Time evolution of plasma current and radial magnetic field amplitudes and phases for different $m = 1$ modes, equilibrium with $\Theta = 1.65$. (a) Plasma current. Mode amplitudes for (b) $n = -11$, (c) $n = -10$, (d) $n = +5$, (e) $n = +6$, and mode phases for the same modes (f) $n = -11$, (g) $n = -10$, (h) $n = +5$, (i) $n = +6$. Three discharges are compared: shot 15 863, without feedback (dotted-dashed line), shot 15 867 with feedback on all modes except $-2 \le n \le +2$ (dashed line) and shot 16 369 with feedback on only the main internal RWMs $-11 \le n \le -8$ (solid line). Mode phases are computed at a feedback active coil position.

modes $n = +5$ and $n = +6$. The $n = +5$ mode amplitude is only slightly suppressed while the $n = +6$ amplitude is strongly decreasing. This behavior can be understood by inspection of the phases for the coupled modes in Fig. 4. The modes $n = (-11, +5)$ are almost in antiphase while the modes $n = (-10, +6)$ are in phase at the positions of the active coils. Since the control fields for the coupled modes are in phase at the active coil positions, simultaneous suppression of coupled modes is effective in the case $n = (-10, +6)$ but not for $n = (-11, +5)$. At around $t = 10$ ms, the $n = +6$ amplitude is close to zero, the mode phase changes so that the mode is in antiphase with the $n = -10$ mode that mainly determines the control field amplitude and phase for this coupled pair, and the $n = +6$ mode begins to grow. The growth rates of modes in the coupled sets are comparable during the later stage of the discharge.

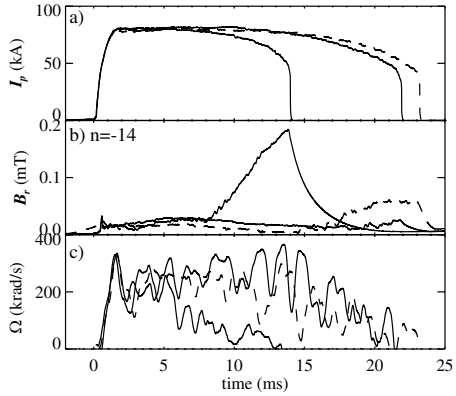


FIG. 5. Time evolution of $n = -14$ resonant mode. (a) plasma current, (b) radial field amplitude, (c) tearing mode rotation angular velocity. Three discharges are compared: shot 15 863, without feedback (dotted-dashed line), shot 15 867 with feedback on all modes except $-2 \leq n \leq +2$ (dashed line) and shot 16 369 with feedback on only the main internal RWMs $-11 \leq n \leq -8$ (solid line).

This behavior is in qualitative agreement with the theoretical modeling, which predicts that complete feedback stabilization of a set of two unstable coupled modes is impossible with the present feedback scheme (that uses the same feedback gain on both modes) [8]. It is expected that, with feedback, the growth rate of the most unstable coupled mode in the set will, at best, be reduced to the value of the growth rate (without feedback) of the next most unstable mode in that same set. In this case, the feedback suppression of the main internal modes $n = -11, -10$ would be limited from below by the growth rates of the external modes $n = +5, +6$.

The negative effect of the coupling on the main modes can be removed by only targeting the internally nonresonant modes for feedback. To clarify the effect of the nonresonant RWMs on the discharge duration, the feedback on other modes including the resonant modes is also avoided. For the second scheme, shown in Fig. 4 (solid line), the same proportional gain is used as in the first case, but applied only to the main unstable internally nonresonant modes $-11 \leq n \leq -8$. A much better suppression of these modes is achieved in this case, especially for $n = -11$. The amplitudes of the main modes $-11 \leq n \leq -8$ remain low, indicating that these modes are more or less completely stabilized by the feedback action. The externally nonresonant RWMs are still affected due to the coupling through the feedback coils.

A significant extension of the pulse length is obtained with feedback. One example where the pulse length increases from 14 ms without feedback to 22–23 ms with feedback is shown in Fig. 4 . Prior to the discharge end, the internally resonant rotating tearing modes lock to the wall, and the amplitudes increase, evidently leading to the discharge termination. Measurement of tearing mode angular rotation frequencies show that wall locking is delayed in discharges with active feedback (Fig. 5). The prolongation of the pulse and the delay of wall locking is also achieved when only the main internally nonresonant RWMs $-11 \leq n \leq -8$ are targeted for feedback, pointing to the existence of a coupling between growth of nonresonant on-axis RWMs and the rotation of the plasma and the tearing modes.

In summary, multiple independent RWMs are simultaneously suppressed for 3–4 wall times using magnetic feedback control with an array of active coils. The feedback experiments are at an early stage, and the feedback system is not optimized. Coupling of different modes are present due to the limited number of active coils, in agreement with theory. Feedback stabilization is indeed successful if there is only one unstable mode in a pair of modes coupled by the coils. When both modes are unstable, there are two possible strategies: partial suppression of both modes or complete stabilization of one target mode while the second mode is left unstable. The present results are encouraging, providing the first successful demonstration of direct magnetic feedback stabilization of multiple RWMs.

[1] A. M. Garofalo *et al.*, Phys. Rev. Lett. **82**, 3811 (1999).
[2] E. J. Strait *et al.*, Phys. Plasmas **11**, 2505 (2004).
[3] M. Okabayashi *et al.*, Phys. Plasmas **8**, 2071 (2001).
[4] C. G. Gimblett, Nucl. Fusion **26**, 617 (1986).
[5] T. C. Hender, C. G. Gimblett, and D. C. Robinson, Nucl. Fusion **29**, 1279 (1989).
[6] Z. X. Jiang and A. Bondeson, Phys. Plasmas **2**, 442 (1995).
[7] C. M. Bishop, Plasma Phys. Controlled Fusion **31**, 1179 (1989).
[8] R. Fitzpatrick and E. P. Yu, Phys. Plasmas **6**, 3536 (1999).
[9] R. Paccagnella, D. D. Schnack, and M. S. Chu, Phys. Plasmas **9**, 234 (2002).
[10] R. Paccagnella, D. Gregoratto, and A. Bondeson, Nucl. Fusion **42**, 1102 (2002).
[11] D. Gregoratto, R. Paccagnella, and Y. Q. Liu, Nucl. Fusion **44**, 1 (2004).
[12] B. Alper *et al.*, Plasma Phys. Controlled Fusion **31**, 205 (1989).
[13] P. Greene and S. Robertson, Phys. Fluids B **5**, 556 (1993).
[14] B. Alper, Phys. Fluids B **2**, 1338 (1990).
[15] P. R. Brunsell *et al.*, Plasma Phys. Controlled Fusion **43**, 1457 (2001).
[16] J.-A. Malmberg and P. R. Brunsell, Phys. Plasmas **9**, 212 (2002).
[17] J.-A. Malmberg *et al.*, Phys. Plasmas **11**, 647 (2004).
[18] P. R. Brunsell *et al.*, Phys. Plasmas **10**, 3823 (2003).
[19] G. Marchiori *et al.*, Fusion Eng. Des. **66-68**, 691 (2003).
[20] O. Barana *et al.*, "Progress in real-time feedback control systems in RFX," in 4th IAEA TCM on Control, Data Acquisition and Remote Participation, San Diego, CA, USA, 21-23 July 2003 (to be published).